New insights into the pathogenesis of Beckwith-Wiedemann and Silver-Russell syndromes: contribution of small copy number variations to 11p15 imprinting defects.

Julie Demars, Sylvie Rossignol, Irène Netchine, Kai Syin Lee, Mansur Shmela, Laurence Faivre, Jacques Weill, Sylvie Odent, Salah Azzi, Patrick Callier, et al.

Contribution of Small Copy Number Variations to The Pathogenesis of Imprinted 11p15-Related Fetal Growth Disorders

Julie Demars,[1] Sylvie Rossignol,[2] Irene Netchine,[2] Kai Syin Lee,[1] Mansur Shmela,[1] Laurence Faivre,[3] Jacques Weill,[4] Sylvie Odent,[5] Salah Azzi,[2] Patrick Callier,[6] Josette Lucas,[7] Christèle Dubourg,[8] Joris Andrieux,[9] Yves Le Bouc,[2] Assam El-Osta,[1] Christine Gicquel,[1]*

[1]Epigenetics in Human Health and Disease, Baker IDI Heart and Diabetes Institute, Melbourne, 3004, Victoria, Australia. [2]APHP, Hôpital Armand Trousseau, Laboratoire d'Explorations Fonctionnelles Endocriniennes, Unité mixte de recherche INSERM UMPC U938, Paris, 75012, France. [3]Centre de Génétique, CHU Dijon, 21033, France. [4]Service d'Endocrinologie pédiatrique, Hôpital Jeanne de Flandre, Lille, 59037, France. [5]Service de Génétique Clinique, CHU Pontchaillou, Rennes, 35203, France. [6]Laboratoire de cytogénétique, CHU Dijon, 21033, France. [7]Laboratoire de cytogénétique, CHU Pontchaillou, Rennes, 35203, France. [8]Laboratoire de génétique moléculaire, CHU Pontchaillou, Rennes, 35203, France. [9]Laboratoire de génétique médicale, Hôpital Jeanne de Flandre, Lille, 59037, France.

Key words: genomic imprinting, copy number variation, 11p15 region, Silver-Russell syndrome, Beckwith-Wiedemann syndrome, fetal growth.

* Correspondence: christine.gicquel@bakeridi.edu.au

Abstract

The imprinted 11p15 region is organized in two domains, each of them under the control of its own imprinting control region (ICR1 for the *IGF2/H19* domain and ICR2 for the *KCNQ1OT1/CDKN1C* domain).

Disruption of 11p15 imprinting results in two fetal growth disorders with opposite phenotypes: the Beckwith-Wiedemann (BWS) and the Silver-Russell (SRS) syndromes. Various 11p15 genetic and epigenetic defects have been demonstrated in BWS and SRS. Among them, isolated DNA methylation defects (ICR1 gain of methylation or ICR2 loss of methylation in BWS and ICR1 loss of methylation in SRS) account for approximately 60% of patients.

To investigate whether cryptic Copy Number Variations (CNVs) involving only part of one of the two imprinted domains account for 11p15 isolated DNA methylation defects, we designed a Single Nucleotide Polymorphism array covering the whole 11p15 imprinted region and genotyped one hundred eighty five SRS or BWS cases with loss or gain of DNA methylation at either ICR1 or ICR2.

We describe herein novel small gain and loss CNVs in six BWS or SRS patients, including maternally-inherited *cis*-duplications involving only part of one of the domains in SRS and BWS patients. We also show that *i*) ICR2 deletions do not account for BWS with ICR2 loss of methylation and *ii*) uniparental isodisomy involving only one of the two imprinted domains is not a mechanism for SRS or BWS.

Those novel defects led new light in the regulation of 11p15 genomic imprinting.

Introduction

Human chromosome 11p15.5 contains a cluster of imprinted genes that play a crucial role in the control of fetal growth [1-4]. This cluster is organized in two neighboring imprinted domains, the *IGF2/H19* and the *KCNQ1OT1/CDKN1C* domains, each of them under the control of its own imprinting control region, ICR1 and ICR2 respectively. Aberrant genomic imprinting of the 11p15 region has a pivotal role in both Beckwith-Wiedemann (BWS; MIM 130650) and Silver-Russell (SRS; MIM 180860) syndromes. BWS is characterized by pre-and/or postnatal overgrowth and other features including hemihyperplasia and an increased risk of childhood tumors. SRS is characterized by severe pre- and postnatal growth retardation, dysmorphic facial features, feeding difficulties and body asymmetry.

Various 11p15 molecular aberrations including genetic and epigenetic abnormalities have been demonstrated in BWS and SRS [5-8]. Among genetic defects, paternal isodisomy of the 11p15 region involving the two imprinted domains is a classical cause of BWS and accounts for 20-25% of BWS cases [5, 9, 10], whereas maternal isodisomy has been reported in only one SRS case [11]. Approximately ten unbalanced translocations (gain CNV) involving both imprinted domains have also been described. When familial, these translocations result in a fetal growth retardation phenotype when maternally-inherited and an overgrowth phenotype when paternally-inherited, as reviewed in [12]. Nevertheless, epigenetic defects (i.e gain or loss of DNA methylation at either ICR1 or ICR2) are very frequent and account for approximately 60-70% of BWS and SRS patients. DNA methylation defects involving ICR2 (loss of methylation) result in BWS (60% of cases) whereas DNA methylation defects involving ICR1 result in both BWS (gain of methylation, 10% of cases) and SRS (loss of methylation, 50-60% of cases) [5-7, 13]. For a small percentage of those patients, the DNA methylation defect is secondary. Mutations/deletions in ICR1 *cis*-regulatory elements account for 20% of BWS patients with ICR1 gain of methylation [14-18], whereas deletions in ICR2 *cis*-regulatory elements in BWS patients have been exceptionally reported [19, 20]. On the other hand, in a subset of BWS patients (25%) with

ICR2 loss of methylation and SRS patients (10%) with ICR1 loss of methylation, the loss of methylation involves imprinted loci other than 11p15 suggesting the dysregulation of an unidentified *trans*-acting factor controlling the establishment and/or the maintenance of genomic imprinting at several loci [21-26]. Altogether, these secondary DNA methylation defects (deletion of a *cis*-regulatory element or involvement of a *trans*-acting regulatory factor) account for a small group of BWS and SRS cases and the mechanism of the DNA methylation defect remains unexplained in most cases.

Conventional diagnostic tools used in 11p15 fetal growth disorders present either a low resolution level (> 500 kb), (*i.e* caryotype, FISH analysis) or high resolution level (< 5 kb), (sequencing, DNA methylation analysis, Multiplex ligation-dependent probe amplification, long-range PCR) and they might fail to recognize intermediate CNVs, ranging from 5 to 500 kb. Assessment of small segmental CNVs has not been systematically addressed in SRS and BWS patients with isolated DNA methylation defects. To investigate whether cryptic CNVs account for 11p15 isolated DNA methylation defects, we designed a customized Single Nucleotide Polymorphism (SNP) array (1536 SNPs) covering the whole 11p15 imprinted region. We genotyped a large series of one hundred eighty five SRS and BWS cases with loss or gain of DNA methylation at either ICR1 or ICR2. We describe herein novel gain and loss CNVs in both BWS and SRS patients.

Subjects and Methods

Subjects

This study was conducted in compliance with institutional guidelines for research studies in human genetics (approval no. 253/07, Alfred Hospital Ethics Committee and agreement numbers 681 and 682, Assistance Publique-Hôpitaux de Paris) and informed consent was obtained from participating individuals and/or their parents. The study population consisted of 50 ethnically matched control subjects and 185 patients with growth disorders caused by a DNA methylation defect of the 11p15 domain. A subset of BWS and SRS patients with abnormal DNA methylation at ICR1 was analyzed in a previous study [18]. Patients with cytogenetic abnormalities, 11p15 parental isodisomy or *CDKN1C* gene mutation and patients with a multilocus imprinting disorder [21; 22] were excluded from the study. Biparental inheritance of the 11p15 region was shown by Southern-blot and/or microsatellite analysis.

One hundred and thirteen patients were diagnosed with BWS. Seventy-eight of them displayed a loss of methylation at ICR2. Thirty-five BWS patients displayed a gain of methylation at ICR1. Nine BWS cases (six with ICR2 loss of methylation and three with ICR1 gain of methylation) were fetal cases (medically terminated pregnancies in 50% of cases and spontaneous abortion in 50% of cases). Five BWS cases were familial forms (one with ICR2 loss of methylation and four cases from two families with ICR1 gain of methylation).

Seventy-two patients were SRS patients who displayed loss of methylation at ICR1.

Parental DNA was available for 110 (59%) BWS or SRS patients. In 93 cases, DNA was available from both parents. Non-paternity was found in three BWS cases with ICR2 loss of DNA methylation and only maternal DNA was considered in those cases.

The clinical and molecular data of BWS and SRS patients are summarized in tables 1 and 2.

Methods

Selection of SNP probes and Oligo Pool Assay design

An Oligo Pool Assay (OPA) of 1536 SNPs covering the whole 11p15

region (location on chromosome 11: position 1,970,084-2,869,522, NCBI 36/hg18 assembly) and including the two imprinted domains was designed. To allow a high success rate of genotyping, only SNPs with an Illumina SNP_score >0.6 were selected among the 6214 polymorphisms present in dbSNP130 and located in the region of interest. SNPs already genotyped in the HapMap CEU population (our disease panel consists mostly of European individuals) were preferentially chosen. They represent 648 SNPs out of the 1536 final dataset. We selected SNPs dispersed homogenously along the domain with a final density of 1 to 3 probes per kilobase. Moreover, regions corresponding to the two imprinting control regions (ICR1 and ICR2) were enriched with a density of one probe every 300 bp. The customized OPA was used to genotype patients, their parents and some of the family members as well as control samples on the iScan System (http://www.illumina.com) according to the manufacturer's protocol.

Preparation of SNP data

We generated a total of ~ 735 000 genotypes in 473 samples. Genotypes were analyzed using the Illumina GenomeStudio software (http://www.illumina.com). After reclustering, 8 samples with a call rate <95% and 340 probes with excessive noise or aberrant clustering patterns (based on the GenTrain Score and manual inspection) were permanently excluded from further analysis. Following a series of quality control steps, an initial design using 1536 SNPs and 473 individuals was reduced to a final dataset of 1196 SNPs and 465 samples (including the 185 patients and 50 control subjects).

CNVs detection by Illumina and QuantiSNP v2.3 softwares

Analysis of CNVs was done based on log R ratio and B allele frequency values issued from the Illumina GenomeStudio and Beadstudio v3.1 softwares. Firstly, we used the cnvPartition v2.4.4 plug-in (http://www.illumina.com) implemented in the Illumina GenomeStudio software to identify CNVs. Given the density of probes in the OPA (one to three per kb), CNVs as small as 1 kb could be potentially detected. We performed a non-stringent analysis considering 3 consecutive probes, a minimum size of 1,000 bp and a threshold of 35 according to the

program. Because the cnvPartition algorithm uses an undocumented method of CNV detection, we also used the QuantiSNP v2.3 software developed by Colella *et al.* [27]. QuantiSNP based on Objective Bayes Hidden-Markov Model treats independently log R ratio and B allele frequency and has been shown to outperform other softwares [28]. The analysis was performed using default parameters [27] and a score (Log Bayes Factor) was assigned to each identified CNV; only CNVs with a stringent threshold score (Log Bayes Factor >30) have been considered. Secondly, to identify runs of homozygosity, we used the Homozygosity Detector plug-in (http://www.illumina.com) implemented in the Illumina BeadStudio v3.1 software as well as the QuantiSNP v2.3 software. The analysis was performed using the default parameters of the Homozygosity Detector program. All regions with more than 50 homozygous and a cutoff significance $\chi 2>23.5$ were marked as runs of homozygosity. For the analysis using the QuantiSNP v2.3 software, only runs of homozygosity with a Log Bayes Factor > 30 were considered.

Validation of identified CNVs by quantitative real-time PCR analysis and CGH array

Quantitative real-time PCR**:** Validation of CNVs identified from the SNP array was performed by quantitative real time PCR. We designed at least 5 primer sets located within and outside the region of interest to confirm the CNVs and map their limits. Quantitative real time PCR was carried out by using a 7500 fast real time PCR system (ABI systems) and Fast SYBR green mix (Roche). Data expressed as the relative quantification were normalized to a region located in the neurogenin 1 gene in which no genetic variation has been described. Two normal individuals were included. All primers used in this study are listed in Supplementary table 1.

CGH array: Validation of some CNVs identified from the SNP array was performed using the 244K Agilent - Human CpG Island Microarray Kit (patient S72P) or the 4x180K Agilent-Human Genome Microarray Kit (patient H47P) (Agilent Technologies, Santa Clara, CA, USA).

Bisulfite sequencing

Bisulfite sequencing was performed as previously described [18]. Primers used in this study are listed in Supplementary table 1.

Karyotyping and FISH characterisation

Chromosomes were prepared from peripheral blood lymphocyte cultures following standard procedures. Fluorescence in situ hybridization (FISH) using chromosome 11 specific subtelomeric probes (patient H47P) was performed according to the manufacturer's specifications (Abbott molecular/Vysis, USA). The BAC probes used in other FISH analyses include RP11-295K3 and RP3-416J11 (patient S72P) and CTD-2242D18 (patient L65P).

Results

Several parameters were used to assess the likelihood of pathogenicity of a CNV in this study: *i*) the specific localization of a CNV within the 11p15 region (*i.e* the CNV involves key regulatory elements such as ICR2 in BWS patients with loss of methylation involving the centromeric domain or ICR1 in BWS and SRS patients with a DNA methylation defect of the telomeric domain). *ii*) the parental transmission of the CNV in familial cases: when inherited, a CNV inherited from a healthy parent was considered as potentially pathogenic. *iii*) copy-neutral CNVs (runs of homozygosity) were considered as potentially pathogenic as losses and gains, as they might reflect segmental uniparental isodisomy. *iv)* variants that are seen in healthy individuals are less likely to account for a patient's phenotype. To this purpose, the database of genomic variants (http://projects.tcag.ca/variation/) was consulted.

New intermediate CNVs in BWS or SRS patients with DNA methylation defect at ICR1 or ICR2

Six CNVs (2 deletions and 4 duplications) were identified in six patients, by using the cnvPartition v2.4.4 and/or the QuantiSNP v2.3 softwares (Table 3). Three CNVs (4 to 22 kb) were only identified with the cnvPartition software and they were not confirmed by quantitative PCR. Three CNVs, all duplications, were identified with both softwares and were confirmed by quantitative real-time PCR. Those three validated duplications were further characterized.

H47P BWS patient:

The male patient was a first child, born after 38 weeks of gestation following ovarian stimulation. Prenatal sonography identified cystic hygroma and unilateral pyelectasis. Antenatal karyotype was normal. There was no familial history of BWS. At birth, the patient displayed severe macrosomia (birth length 56 cm, +3.4 SD; birth weight 5490 g, +5.9 SD), macroglossia, umbilical hernia and facial dysmorphia and the first months of post-natal life were marked by feeding difficulties. In early post-natal life, the patient was diagnosed with developmental delay, expressed primarily in the form of hypotonia and non-specific speech retardation. He walked at the age of 17 months. He underwent pyeloplasty for

ureteropyelic junction stenosis at the age of 1 year and glossoplasty at the age of 3 years. Physical examination at the age of $5^{1/12}$ years showed a slight asymmetry of the face, lower limbs and kidneys and advanced growth (+3.5 SD for height and +4.5 SD for weight).

Analysis of the 11p15 region showed a partial gain of methylation at ICR1 [methylation index at 72% (normal: 53.9 ± 2%)] with a normal methylation status at ICR2 [methylation index at 45% (51.6 ± 2.5%)]. Analysis of SNP array data (Log R Ratio and B allele frequency) identified a duplication (Figure 1A). The duplication covered the whole *IGF2/H19* domain, involving the most telomeric probe (position 1,970,084, NCBI36/hg18 Assembly), with a centromeric breakpoint located within the 3' end of the *CD81* gene (between position 2,374,469 and 2,375,108). Quantitative PCR showed that the duplication extends to the telomeric end of the short arm (Figure 1B) refining the size of the duplication to approximately 2.4 Mb. SNP analysis showed that the duplication involved the paternal allele (Figure 1C). CGH array confirmed the telomeric duplication at 11p15.5 and also identified a 2 Mb telomeric deletion at 11q25 (breakpoint between position 132,431,292 and 134,432,465) (Figure 1D). Metaphase FISH analysis of H47P with a 11p subtelomeric probe showed signals at both telomeres of a derivative chromosome 11, whereas FISH analysis using a 11q subtelomeric probe confirmed a deletion of 11qter by showing a fluorescent signal on the normal chromosome 11 only (Figure 1E). FISH analysis in parents identified a pericentric inversion in the father, with the 11p subtelomeric probe hybridizing the end of 11q and the 11q subtelomeric probe hybridizing the end of 11p on the inverted chromosome (Figure 1E). As the size of the inverted segment is in the range of 130 Mb, the karyotypes were considered as normal in both H47P and his father (data not shown). This observation shows that partial trisomy 11p15 and partial monosomy 11q25 in H47P resulted from unequal crossing over during paternal meiosis.

S72P SRS patient:

The female patient was the second child, conceived naturally from non consanguineous parents (Figure 2A). At birth (term of 36 weeks), she displayed intrauterine growth retardation [birth weight of 1690 g (-2.6 SD),

birth length of 39.5 cm (-4.4 SD)] with relative macrocephaly (-0.4 SD). Early postnatal life was marked by severe feeding difficulties and growth deceleration (-3 SD at the age by 7 months and -3.7 SD by the age of 15 months) with a BMI of – 2 SD. SRS was diagnosed during the second year of life on the basis of postnatal growth retardation with conserved head circumference, bossed forehead, clinodactyly of the fifth digits, body asymmetry and feeding difficulties. The parents and the older brother were clinically normal and there was no familial history of SRS on the maternal side.

Analysis of the 11p15 region showed a partial loss of methylation at ICR1 (methylation index at 25%) with a normal methylation status at ICR2 (methylation index at 47%). Analysis of SNP array data identified a maternally-inherited duplication covering part of the *IGF2/H19* domain, including the *H19* gene and ICR1 but not the *IGF2* gene (Figure 2B). Characterization of the duplication by quantitative PCR and CGH array estimated its size between 562 and 575 kb with the telomeric breakpoint located between 1,522,259 and 1,530,602 bp (within the *HCCA2* gene) and the centromeric breakpoint located between 2,092,578 and 2,097,357 bp (Figures 2C and 2D). Two color FISH analysis of S72P and her mother with two BAC probes (RP11-295K3 within the duplication and RP3-416J11 outside the duplication) excluded an unbalanced translocation and showed an increased signal at 11p with RP11-295K3, providing indirect evidence for *cis*-duplication of the affected region (Figure 2E). FISH on S72P's interphased nuclei clearly showed three hybridization signals confirming the *cis*-duplication (Figure 2F). Methylation analysis in the mother showed a gain of methylation at ICR1 (methylation index at 68%). The mother's phenotype was normal and no clinical history in early childhood was indicative of BWS. Both maternal grandparents had normal phenotypes and there was no familial history suggesting SRS or BWS cases. Assuming that the grand paternal allele was methylated in the mother, we performed genomic and bisulfite sequencing of the ICR1 B6 repeat (1,980,297-1,980,616 bp) in S72P and her mother. An allelic imbalance was observed for the informative rs61383602 SNP in the mother, suggesting that the C allele was the duplicated allele (Figure 2 G). Bisulfite

sequencing showed that in the mother, the duplicated C allele peak was methylated confirming that the duplication originated from the maternal grandfather (Figure 2G).

Familial L65P BWS case: The family was previously reported as a clinical description in 1983 [29]. All the affected subjects were conceived from normal sisters (Figure 3A). Patient L65P (III.7, Figure 3A) was born after 40 weeks of a normal gestation from non consanguineous parents. The clinical presentation at birth included macroglossia, exomphalos, hypospadias, bilateral cryptorchidism, bilateral inguinal hernias, posterior helical pits and severe neonatal hypoglycemia. Patient L65P had no macrosomia at birth (birth weight 3200 gr, -0.6 SD) but then displayed advanced growth (+ 2.5 SD at the age of 5 years) with a final height at 196 cms (+ 2.8 SD). The familial history includes three other cases. The first pregnancy of individual II.1 was complicated at five months of gestation by acute hydramnios resulting in fetal death. Pathologic findings of the male fetus (III.1) included exomphalos, adrenal cytomegaly and leydigian hyperplasia. A second pregnancy was terminated after 25 weeks of gestation after ultrasound examination showed an exomphalos. The first pregnancy of individual II.4 was also terminated after 18 weeks of gestation after ultrasound diagnosis of exomphalos. Pathologic findings of the female fetus (III.8) included exomphalos, adrenal cytomegaly and ovarian hyperplasia. A second pregnancy resulted in spontaneous abortion at 9 weeks. Analysis of the 11p15 region showed a complete loss of methylation at ICR2 in patient III.7 whereas the ICR2 methylation status in the mother (II.3) and her two sisters (II.1 and II.4), obligate carriers, was normal (Figure 3B). The ICR2 methylation pattern was also normal in the individuals whom DNA was available, including the maternal grandmother (Figure 3B). Search for a deletion involving ICR2 was negative (PCR and quantitative PCR) and this hypothesis was unlikely as the ICR2 DNA methylation profile was normal in L65P's mother and her sisters. ICR2 was also sequenced (position 2,677,063 to 2,679,536 bp) and no small deletions or mutations were identified.

Analysis of SNP array and Log R Ratio data identified an approximately 50 kb duplication ranging from approximately 2,485,000 to 2,533,000 bp

(Figure 3C), involving the 3' part of intron 1, exon 2 and 5' part of intron 2 of the *KCNQ1* gene (isoform NM000218.2). The duplication was confirmed by quantitative PCR with the telomeric breakpoint located between 2,472,581 and 2,486,398 bp and the centromeric breakpoint located between 2,526,347 and 2,540,424 bp (Figure 3D). The duplication was also found in the three sisters (obligate carriers) and also in unaffected individuals II.5 and III.5. Subject I.1 did not display the duplication (Figures 3C and 3D), suggesting that the duplication was transmitted from L65P's maternal grandfather (DNA not available) to the five siblings (II.1 to II.5). The duplication was also absent in the only unaffected child (III.3) born from one (II.1) of the three sisters (Figures 3A and 3D). FISH analysis with the CTD-2242D18 probe (position: 2,469,461-2,575,865) did not detect an increased hybridization signal on chromosome 11. It is likely that the small size of the duplication prevented its identification by FISH. The absence of an extra signal on another chromosome is in favor of a 11p15 *cis*-duplication.

As the duplication encompasses two CpG islands, we investigated the methylation status of those CpG islands in three control subjects, L65P, his mother (II.3) and his maternal grandmother (I.1). Bisulfite sequencing analysis of the CpG island in position 2,510,680-2,510,907 showed that both parental alleles were unmethylated (Figure 3F) in control subjects, patient L65P and subjects II.3 and I.1. Analysis of the CpG island in position 2,511,982-2,512,194 showed that the CpG island was predominantly methylated with no allele-specific DNA methylation in controls (Figure 3F). In patient L65P, subjects II.3 and I.1, the DNA methylation pattern was the same as in control subjects.

Small CNVs in BWS patients with gain of DNA methylation at ICR1

A few ICR1 deletions have been previously reported, essentially in BWS patients. They are small in the range of 1-2 kb and as they involve very few markers, they might be missed by the CNV detection methods. We therefore performed an accurate analysis of respective imprinting control regions in patients with abnormal DNA methylation at ICR1 or ICR2, assuming that homozygous calls (B allele frequency) with a reduced copy

number (log R ratio) for SNPs mapping to ICR1 (1,976,000-1,981,000 bp) or ICR2 (2,676,000-2,679,000 bp) will reflect the occurence of a hemizygous deletion.

Three BWS patients with ICR1 gain of methylation displayed a low log R ratio for two or three SNPs located within ICR1 (Figure 4A). Two of them, H32P (previously reported, [18]) and H50P presented as apparently sporadic BWS cases. H63P had a familial history of Wilms tumors on the maternal side (Figure 4B). H63P's mother herself displayed a phenotype indicative of BWS, including macrosomia at birth, organomegaly and body asymmetry. She also developed a Wilms tumor when she was 5 years old. Deletions were characterized by long range PCR, quantitative PCR and sequencing (Figures 4C, 4D and 4E). All deletions were maternally-inherited (Figure 4C). The two 1834 bp deletions (H32P and H50P) fusion blocks B6 with B3, removing two CTCF binding sites but involve different breakpoints (Figure 4F and Table 4). The 2240 bp H63P deletion fusions blocks B6 with B2 and removes CTCF binding sites 2, 3 and 4 (Figures 4E, 4F and Table 4).

No ICR1 deletion was detected in a series of 72 SRS patients displaying ICR1 loss of methylation. Similarly, investigation of a large series of 78 BWS with ICR2 loss of methylation did not identify any deletion.

Copy neutral CNVs

Copy neutral CNVs correspond to runs of homozygosity without any change in copy number. They might reflect uniparental isodisomy (UPiD) or autozygosity. UPiDs previously identified in BWS and SRS patients involve both ICR1 and ICR2 and display a mosaic pattern. The density of the SNP array and the availability of parental DNA for 60% of patients made possible the identification of segmental UPiDs. Analysis of the data for shift in B allele frequency for heterozygous SNPs (not centered at 0.5), associated with a normal log R ratio and mendelian inconsistency (when parental DNA was available) did not identify mosaic segmental UPiD in SRS or BWS patients with loss or gain of DNA methylation at either ICR1 or ICR2.

However, runs of homozygosity, ranging from 86 to 335 kb (156 to 592

probes) were identified in the various groups of patients and controls (Figure 5). Although runs of homozygosity were identified within the whole 11p15 region, two locations were overrepresented after analysis with the two softwares. The first region (position 2,170,000 to 2,270,000 bp), encompassing the paternally-imprinted *ASCL2* gene, was homozygous in 17% of both patients and controls (Box A in Figure 5 and supplementary Table 2). The second region (position 2,270,000 to 2,370,000 bp), encompassing the *C11ORF21* and *TSPAN32* genes, was homozygous in 23% and 15% of patients and controls respectively (Box B in Figure 5 and supplementary Table 2).

Discussion

Recent modifications to SNP arrays enhance the opportunity to discover CNVs along with concomitant SNP genotypes. We designed a custom SNP array to target the analysis to the 11p15 region including the two imprinting control regions and investigate whether intermediate lesions (which cannot be recognized by routine diagnostic tools) account for a subset of 11p15 growth disorders with abnormal DNA methylation at either ICR1 or ICR2. A SNP array was favored to CGH array as it has the ability to (*i)* simultaneously measure both intensity differences and allelic ratios and therefore to investigate both DNA copy-number and copy-neutral variation and (*ii)* identify the parental origin of CNVs.

- We identified three novel duplications which have not been previously described.

Two duplications involved the *IGF2/H19* domain. In the H47P BWS case, CGH showed that a 2 Mb deletion of the distal part of 11q was associated with an apparently *de novo* 2.4 Mb duplication of the whole *IGF2/H19* domain on the paternal chromosome. FISH analysis of H47P and his parents demonstrated that H47P displayed recombination of a paternally-inherited pericentric inversion of chromosome 11, with a large inverted segment of approximately 130 Mb (i.e more than 95% of the chromosome). A few 11p pericentric inversions have been previously described [30-32], some of them with a predominant BWS phenotype [30]. Those previously described pericentric inversions led to the duplication of the whole 11p15 imprinted domain with breakpoints between 11p13 and 11p15.1. The H47P case is unique as the duplication of the short arm involves only part of the 11p15 imprinted region (*i.e* the *IGF2/H19* domain). The deletion of 11q25 involves 10 genes and might account for the developmental delay.

The second duplication of the *IGF2/H19* domain represents the first observation of a genetic abnormality within the *IGF2/H19* domain in SRS. The S72P *cis*-duplication involves only part of the *IGF2/H19* domain (the imprinting control region and the *H19* gene) and results in a SRS phenotype only if maternally-inherited when there is no phenotype upon paternal transmission. Both the parental transmission pattern and the

phenotype are different from previously reported ICR1 duplications [12, 33, 34]. *Cis*-duplications (0.3 to 1.8 Mb in size) involving the whole *IGF2/H19* domain have been previously reported in two familial [12, 34] and one sporadic [33] BWS cases. They resulted in a BWS only if the paternal chromosome was involved. The main difference between the S72P duplication and other duplications of the *IGF2/H19* domain ([12, 33, 34] and the H47P case) is that the S72P duplication involves ICR1 and the *H19* gene but does not involve the *IGF2* gene. Hence, a partial maternal *cis*-duplication of the *IGF2/H19* domain results in a SRS phenotype (S72P case) whereas a maternal *cis*-duplication involving the whole *IGF2/H19* domain does not result in any phenotype [12] (Supplementary figure 1). Although two copies of the active maternal *H19* gene are expressed in both cases, the chromatin organization is likely to be different. In the partial *cis*-duplication, one maternal *H19* gene is not engaged in a *cis*-effect. It was recently shown that, apart from a *cis*-effect, the *H19* non-coding RNA also regulates the expression of *Igf2* by a *trans*acting mechanism [35]. Indeed, *H19* transgenic expression is able to rescue the overgrowth phenotype of mice with targeted deletions of the *H19* gene and also to reduce *Igf2* expression [35]. We hypothesize that an extra copy of a functional maternal *H19* gene (not engaged in a *cis*-effect) can affect the expression of *IGF2* by a *trans*acting mechanism and result in growth retardation. Two deletions within or overlapping the S72P duplicated region have been registered as rare variations, in apparently normal subjects (http://projects.tcag.ca/variation/; variations 29891, 29893), but the parental origin of these deletions are not known.

The third duplication case is a familial BWS case with ICR2 loss of methylation, involving four affected subjects conceived from three phenotypically normal sisters. The pattern of transmission of this *cis*-duplication supports its pathogenicity with no phenotype when the duplication is transmitted through the male germline and a BWS phenotype when the duplication is transmitted through the female germline. Moreover, the absence of the duplication in an unaffected subject born from a female carrier strengthens the significance of the duplication. Little is known on the centromeric 11p15 imprinting region

apart from the ICR2 imprinting control region. One deletion within the L65P duplicated region has been registered as a rare variation (http://projects.tcag.ca/variation/; variation 29897) but the parental origin of this deletion is not known. Nevertheless, the 50 kb *cis*-duplication region displays evidence of open chromatin and encompasses two CpG islands and three CTCF binding sites. Analysis of the DNA methylation status of the two CpG islands had not been previously documented. Those two CpG islands are not allele-specific differentially methylated in control subjects, with one being predominantly methylated and the other one unmethylated. In the patient displaying the *cis*-duplication, we showed that the pattern of DNA methylation was similar to the pattern of control subjects. The location of the duplication also corresponds to the centromeric breakpoint of a 1.8 Mb *cis*-duplication responsible for a BWS [33] and the Tm87-16 rhabdoid tumor translocation breakpoint within BWSCR1 [36, 37]. All together, this data strongly supports the relevance of the *cis*-duplication in the BWS phenotype and suggests that the *cis*-duplication affects the chromatin conformation and impairs the apposition and/or maintenance of DNA methylation at ICR2.

- Precise analysis of the two imprinting control regions (ICR1 and ICR2) led to the identification of new small deletions. Those deletions were only identified in BWS patients with ICR1 gain of methylation. As for previous identified deletions [18], the deletion breakpoints in those new cases map repetitive sequences within the B repeats of ICR1, suggesting that these repetitive sequences within ICR1 promote the risk of deletion. No ICR1 deletions were identified in SRS patients with ICR1 loss of methylation and this agrees with previous publications which show the absence of phenotype upon paternal transmission of ICR1 deletions [14, 16]. Moreover, we did not identify ICR2 deletions in this large series of BWS patients with ICR2 loss of methylation. Although ICR2 deletions (0.25 and 0.9 Mb) have been occasionally reported in BWS with loss of methylation at ICR2 [19, 20], the data presented here establishes that they are extremely rare.

- A major advantage of the SNP array is the possibility to combine detection of gain/loss CNVs with copy-neutral CNVs (runs of homozygosity). Such segments of homozygosity could represent

uniparental isodisomy or autozygosity. Uniparental isodisomy is a classical cause of BWS and accounts for 20 to 25% of BWS cases [5 9, 10], whereas maternal isodisomy has been reported in only one SRS case [11]. When the frequency of uniparental isodisomy is well established in BWS, its extent on chromosome 11 has not been extensively analyzed. In a recent study, Cooper et *al.* showed that the extent of isodisomy along chromosome 11 is variable but always involves the two 11p15.5 imprinted domains [10]. In this study, we investigated for the first time whether smaller uniparental isodisomies, confined to one of the two 11p15 imprinted domains, might account for DNA methylation defects restricted to ICR1 or ICR2. Although we identified runs of homozygosity in BWS and SRS patients, the B allele frequency was not indicative of mosaicism and there was no mendelian inconsistency when parental DNA was available. This data shows that segmental uniparental isodisomies confined to the *IGF2/H19* or the *KCNQ1OT1/CDKN1C* domains do not account for DNA methylation defects restricted to one of the two 11p15 imprinted domains.

In summary, investigation by SNP array of a large series of BWS and SRS patients with isolated ICR1 or ICR2 DNA methylation defects led to the identification of new molecular defects including novel segmental *cis*-duplications in both SRS and BWS patients and new ICR1 deletions in BWS patients. This study also establishes, for the first time, that segmental uniparental isodisomies do not account for isolated ICR1 or ICR2 DNA methylation defects. We also demonstrate in a large series of BWS patients that ICR2 deletions are not a common mechanism for loss of methylation at ICR2.

Our data also illustrates the difficulty of genetic counseling in patients with 11p15 related growth disorders. Indeed, in more than 50% of cases, the clinical presentation was sporadic rather than familial despite a maternally-inherited genetic defects. This study and a previous one [18] also emphasize that molecular defects in *cis* are more common than initially thought in BWS patients with ICR1 gain of methylation and affect at least 20% of cases.

Supplemental Data:

Supplemental Data include one figure and two tables and can be found

online at http://www.

Acknowledgments:

We thank Annick Blaise for her technical assistance and the physicians for patients' referrals and collection of clinical data. We are grateful to the willingness of the patients and their families to contribute to this study.

Funding:

This work was supported by the National Health and Medical Research Council of Australia (Project grant 472637), the Baker IDI Heart and Diabetes Institute, the Institut National de la Santé et de la Recherche Médicale UMPC U938, Université Pierre et Marie Curie Paris 6 and Assistance Publique Hopitaux de Paris.

Conflict of interest statement. None declared.

Web Resources:

The URLs for data presented herein are as follows:

Online Mendelian Inheritance in Man (OMIM), http://www.ncbi.nlm.nih.gov/Omim/; International HapMap Project: http://www.hapmap.org/; Database of genomic variants: http://projects.tcag. ca/variation; UCSC Genome Browser, March 2006 build, http://genome. cse.ucsc.edu/

References:

1. Reik, W., and Walter, J. (2001). Genomic imprinting: parental influence on the genome. Nat Rev Genet *2*, 21-32.

2. Delaval, K., and Feil, R. (2004). Epigenetic regulation of mammalian genomic imprinting. Curr Opin Genet Dev *14*, 188-195.

3. Gicquel, C., and Le Bouc, Y. (2006). Hormonal regulation of fetal growth. Horm Res *65 Suppl 3*, 28-33.

4. Hudson, Q.J., Kulinski, T.M., Huetter, S.P., and Barlow, D.P. (2010). Genomic imprinting mechanisms in embryonic and extraembryonic mouse tissues. Heredity. *105,* 45-56.

5. Gaston, V., Le Bouc, Y., Soupre, V., Burglen, L., Donadieu, J., Oro, H., Audry, G., Vazquez, M.P., and Gicquel, C. (2001). Analysis of the methylation status of the KCNQ1OT and H19 genes in leukocyte DNA for the diagnosis and prognosis of Beckwith-Wiedemann syndrome. Eur J Hum Genet *9*, 409-418.

6. Cooper, W.N., Luharia, A., Evans, G.A., Raza, H., Haire, A.C., Grundy, R., Bowdin, S.C., Riccio, A., Sebastio, G., Bliek, J., et al. (2005). Molecular subtypes and phenotypic expression of Beckwith-Wiedemann syndrome. Eur J Hum Genet *13*, 1025-1032.

7. Gicquel, C., Rossignol, S., Cabrol, S., Houang, M., Steunou, V., Barbu, V., Danton, F., Thibaud, N., Le Merrer, M., Burglen, L., et al. (2005). Epimutation of the telomeric imprinting center region on chromosome 11p15 in Silver-Russell syndrome. Nat Genet *37*, 1003-1007.

8. Weksberg, R., Shuman, C., and Beckwith, J.B. (2010). Beckwith-Wiedemann syndrome. Eur J Hum Genet *18*, 8-14.

9. Henry, I., Bonaiti-Pellie, C., Chehensse, V., Beldjord, C., Schwartz, C., Utermann, G., and Junien, C. (1991). Uniparental paternal disomy in a genetic cancer-predisposing syndrome. Nature *351*, 665-667.

10. Cooper, W.N., Curley, R., Macdonald, F., and Maher, E.R. (2007). Mitotic recombination and uniparental disomy in Beckwith-Wiedemann syndrome. Genomics *89*, 613-617.

11. Bullman, H., Lever, M., Robinson, D.O., Mackay, D.J., Holder, S.E., and Wakeling, E.L. (2008). Mosaic maternal uniparental disomy of chromosome 11 in a patient with Silver-Russell syndrome. J Med Genet *45*, 396-399.

12. Bliek, J., Snijder, S., Maas, S.M., Polstra, A., van der Lip, K., Alders, M., Knegt, A.C., and Mannens, M.M. (2009). Phenotypic discordance upon paternal or maternal transmission of duplications of the 11p15 imprinted regions. Eur J Med Genet *52*, 404-408.

13. Netchine, I., Rossignol, S., Dufourg, M.N., Azzi, S., Rousseau, A., Perin, L., Houang, M., Steunou, V., Esteva, B., Thibaud, N., et al. (2007). 11p15 imprinting center region 1 loss of methylation is a common and specific cause of typical Russell-Silver syndrome: clinical scoring system and epigenetic-phenotypic correlations. J Clin Endocrinol Metab *92*, 3148-3154.

14. Sparago, A., Cerrato, F., Vernucci, M., Ferrero, G.B., Silengo, M.C., and Riccio, A. (2004). Microdeletions in the human H19 DMR result in loss of IGF2 imprinting and Beckwith-Wiedemann syndrome. Nat Genet *36*, 958-960.

15. Prawitt, D., Enklaar, T., Gartner-Rupprecht, B., Spangenberg, C., Oswald, M., Lausch, E., Schmidtke, P., Reutzel, D., Fees, S., Lucito, R., et al. (2005). Microdeletion of target sites for insulator protein CTCF in a chromosome 11p15 imprinting center in Beckwith-Wiedemann syndrome and Wilms' tumor. Proc Natl Acad Sci U S A *102*, 4085-4090.

16. Sparago, A., Russo, S., Cerrato, F., Ferraiuolo, S., Castorina, P., Selicorni, A., Schwienbacher, C., Negrini, M., Ferrero, G.B., Silengo, M.C., et al. (2007). Mechanisms causing imprinting defects in familial Beckwith-Wiedemann syndrome with Wilms' tumour. Hum Mol Genet *16*, 254-264.

17. Scott, R.H., Douglas, J., Baskcomb, L., Huxter, N., Barker, K., Hanks, S., Craft, A., Gerrard, M., Kohler, J.A., Levitt, G.A., et al. (2008). Constitutional 11p15 abnormalities, including heritable imprinting center mutations, cause nonsyndromic Wilms tumor. Nat Genet *40*, 1329-1334.

18. Demars, J., Shmela, M.E., Rossignol, S., Okabe, J., Netchine, I., Azzi, S., Cabrol, S., Le Caignec, C., David, A., Le Bouc, Y., et al. (2010). Analysis of the IGF2/H19 imprinting control region uncovers new genetic defects, including mutations of OCT-binding sequences, in patients with 11p15 fetal growth disorders. Hum Mol Genet *19*, 803-814.

19. Niemitz, E.L., DeBaun, M.R., Fallon, J., Murakami, K., Kugoh, H., Oshimura, M., and Feinberg, A.P. (2004). Microdeletion of LIT1 in familial Beckwith-Wiedemann syndrome. Am J Hum Genet *75*, 844-849.

20. Zollino, M., Orteschi, D., Marangi, G., De Crescenzo, A., Pecile, V., Riccio,

A., and Neri, G. (2010). A case of Beckwith-Wiedemann syndrome caused by a cryptic 11p15 deletion encompassing the centromeric imprinted domain of the BWS locus. J Med Genet *47,* 429-432.

21. Rossignol, S., Steunou, V., Chalas, C., Kerjean, A., Rigolet, M., Viegas-Pequignot, E., Jouannet, P., Le Bouc, Y., and Gicquel, C. (2006). The epigenetic imprinting defect of patients with Beckwith-Wiedemann syndrome born after assisted reproductive technology is not restricted to the 11p15 region. J Med Genet *43*, 902-907.

22. Azzi, S., Rossignol, S., Steunou, V., Sas, T., Thibaud, N., Danton, F., Le Jule, M., Heinrichs, C., Cabrol, S., Gicquel, C., et al. (2009). Multilocus methylation analysis in a large cohort of 11p15-related foetal growth disorders (Russell Silver and Beckwith Wiedemann syndromes) reveals simultaneous loss of methylation at paternal and maternal imprinted loci. Hum Mol Genet *18,* 4724-4733.

23. Bliek, J., Alders, M., Maas, S.M., Oostra, R.J., Mackay, D.M., van der Lip, K., Callaway, J.L., Brooks, A., van 't Padje, S., Westerveld, A., et al. (2009). Lessons from BWS twins: complex maternal and paternal hypomethylation and a common source of haematopoietic stem cells. Eur J Hum Genet *17*, 1625-1634.

24. Bliek, J., Verde, G., Callaway, J., Maas, S.M., De Crescenzo, A., Sparago, A., Cerrato, F., Russo, S., Ferraiuolo, S., Rinaldi, M.M., et al. (2009). Hypomethylation at multiple maternally methylated imprinted regions including PLAGL1 and GNAS loci in Beckwith-Wiedemann syndrome. Eur J Hum Genet *17*, 611-619.

25. Lim, D., Bowdin, S.C., Tee, L., Kirby, G.A., Blair, E., Fryer, A., Lam, W., Oley, C., Cole, T., Brueton, L.A., et al. (2009). Clinical and molecular genetic features of Beckwith-Wiedemann syndrome associated with assisted reproductive technologies. Hum Reprod *24*, 741-747.

26. Meyer, E., Lim, D., Pasha, S., Tee, L.J., Rahman, F., Yates, J.R., Woods, C.G., Reik, W., and Maher, E.R. (2009). Germline mutation in NLRP2 (NALP2) in a familial imprinting disorder (Beckwith-Wiedemann Syndrome). PLoS Genet *5*, e1000423.

27. Colella, S., Yau, C., Taylor, J.M., Mirza, G., Butler, H., Clouston, P., Bassett, A.S., Seller, A., Holmes, C.C., and Ragoussis, J. (2007). QuantiSNP:

an Objective Bayes Hidden-Markov Model to detect and accurately map copy number variation using SNP genotyping data. Nucleic Acids Res *35*, 2013-2025.

28. Dellinger, A.E., Saw, S.M., Goh, L.K., Seielstad, M., Young, T.L., and Li, Y.J. (2010). Comparative analyses of seven algorithms for copy number variant identification from single nucleotide polymorphism arrays. Nucleic Acids Res *38*, e105.

29. Nivelon-Chevallier, A., Mavel, A., Michiels, R., and Bethenod, M. (1983). [Familial Wiedeman-Beckwith syndrome: prenatal echography diagnosis and histologic confirmation]. J Genet Hum *31 Suppl 5*, 397-402.

30. Waziri, M., Patil, S.R., Hanson, J.W., and Bartley, J.A. (1983). Abnormality of chromosome 11 in patients with features of Beckwith-Wiedemann syndrome. J Pediatr *102*, 873-876.

31. Stratakis, C.A., Turner, M.L., Lafferty, A., Toro, J.R., Hill, S., Meck, J.M., and Blancato, J. (2001). A syndrome of overgrowth and acromegaloidism with normal growth hormone secretion is associated with chromosome 11 pericentric inversion. J Med Genet *38*, 338-343.

32. Gadzicki, D., Baumer, A., Wey, E., Happel, C.M., Rudolph, C., Tonnies, H., Neitzel, H., Steinemann, D., Welte, K., Klein, C., et al. (2006). Jacobsen syndrome and Beckwith-Wiedemann syndrome caused by a parental pericentric inversion inv(11)(p15q24). Ann Hum Genet *70*, 958-964.

33. Russo, S., Finelli, P., Recalcati, M.P., Ferraiuolo, S., Cogliati, F., Dalla Bernardina, B., Tibiletti, M.G., Agosti, M., Sala, M., Bonati, M.T., et al. (2006). Molecular and genomic characterisation of cryptic chromosomal alterations leading to paternal duplication of the 11p15.5 Beckwith-Wiedemann region. J Med Genet *43*, e39.

34. Algar, E.M., St Heaps, L., Darmanian, A., Dagar, V., Prawitt, D., Peters, G.B., and Collins, F. (2007). Paternally inherited submicroscopic duplication at 11p15.5 implicates insulin-like growth factor II in overgrowth and Wilms' tumorigenesis. Cancer Res *67*, 2360-2365.

35. Gabory, A., Ripoche, M.A., Le Digarcher, A., Watrin, F., Ziyyat, A., Forne, T., Jammes, H., Ainscough, J.F., Surani, M.A., Journot, L., et al. (2009). H19 acts as a trans regulator of the imprinted gene network controlling growth in mice. Development *136*, 3413-3421.

36. Lee, M.P., Hu, R.J., Johnson, L.A., and Feinberg, A.P. (1997). Human KVLQT1 gene shows tissue-specific imprinting and encompasses Beckwith-Wiedemann syndrome chromosomal rearrangements. Nat Genet *15*, 181-185.
37. Prawitt, D., Enklaar, T., Klemm, G., Gartner, B., Spangenberg, C., Winterpacht, A., Higgins, M., Pelletier, J., and Zabel, B. (2000). Identification and characterization of MTR1, a novel gene with homology to melastatin (MLSN1) and the trp gene family located in the BWS-WT2 critical region on chromosome 11p15.5 and showing allele-specific expression. Hum Mol Genet *9*, 203-216.
38. Schonherr, N., Meyer, E., Roos, A., Schmidt, A., Wollmann, H.A., and Eggermann, T. (2007). The centromeric 11p15 imprinting centre is also involved in Silver-Russell syndrome. J Med Genet *44*, 59-63.

Figures titles and legends:

Figure 1: ICR1 duplication resulting from recombination of a paternal pericentric inversion in a BWS patient with ICR1 gain of methylation

(**A**) Graphical overview of B allele frequency and log R Ratio obtained from the SNP array in H47P and his parents, showing a duplication of the *IGF2/H19* domain in H47P. The location of the duplication is highlighted by the grey box. (**B**) Genomic real-time PCR quantification assay at various loci along the *IGF2/H19* domain validating the duplication. (**C**) Sequencing at various informative SNPs within the duplication showing that the duplication involves the paternally-inherited allele. (**D**) Graphical overview of the results obtained from the array-CGH analysis of H47P, showing a distal 11p duplication and a distal 11q deletion. (**E**) FISH analysis with subtelomeric probes for 11p (green) and 11q (red). The normal chromosome 11 has one green and one red signal for 11p and 11q, respectively. In H47P, the recombinant chromosome 11 [rec(11) dup p inv(11)] has green signals for 11p on both ends and no red signal. In H47P's father, the inverted chromosome 11 [inv(11) p15.5q25] has a red signal on 11p and a green signal on 11q. Small white arrows indicate the centromeres.

Figure 2: Familial ICR1 duplication in a SRS patient with ICR1 loss of methylation

(**A**) Pedigree of the S72P SRS case. (**B**) Graphical overview of B allele frequency and log R Ratio obtained from the SNP array in S72P and her parents, showing a maternally-inherited segmental duplication of part of the *IGF2/H19* domain in S72P. The location of the duplication is highlighted by the grey box. (**C**) Genomic real-time PCR quantification assay at various loci along the *IGF2/H19* domain validating the duplication in S72P and her mother. (**D**) Graphical overview of the results obtained from the array-CGH analysis of S72P. The duplication interval (from 1,530,602 to 2,092,578 bp) is underlined with the pink rectangle. (**E**) Partial metaphases of patient S72P. FISH with the BAC probe RP11-295K3 within the duplication shows an increased hybridization signal (green signal) on one of the chromosomes 11 (arrow) when the signal with the BAC probe RP3-416J11 outside the duplication (red signal) is similar

on both chromosomes. (**F**) FISH on S72P's interphased nuclei with the BAC probe RP11-295K3 shows three hybridization signals confirming the duplication. (**G**) Chromatograms of the ICR1 B6 repeat including SNP rs61383602 (framed in red) before and after bisulfite treatment for patient S72P and her mother. After bisulfite treatment, patient S72P (non informative for the polymorphism) displays a T allele peak (unmethylated duplicated maternal allele) higher than the C allele peak (methylated paternal allele). In the mother, informative for the polymorphism, before treatment by bisulfite, the C allele peak is higher than the T allele confirming the duplication. The profile is the same after bisulfite treatment showing that the C methylated allele was inherited from the maternal grandfather.

Figure 3: Familial ICR2 BWS case

(**A**) Pedigree of the familial BWS case and segregation. Subjects identified with the duplication are indicated with a star. SB: stillbirth. (**B**) DNA methylation at ICR2, assayed by methyl-sensitive Southern blotting using genomic DNA from the indicated individuals. The upper band (6 kb) is methylated and corresponds to the maternal allele. The lower band (4.2 kb) is unmethylated and corresponds to the paternal (ICR2) allele. (**C**) Graphical overview of log R Ratio results obtained from the SNP array in L65P (III.7), his mother (II.3) and maternal grandmother (I.1), showing a maternally-inherited duplication in L65P and his mother. The location of the duplication is highlighted by the grey box. (**D**) Genomic real-time PCR quantification assay at several loci along the ICR2 domain validating the duplication. (**E**) DNA methylation profiles of the two CpG islands included in the *cis*-duplication determined by bisulfite sequencing in a control subject, the propositus (L65P/III.7), his mother (II.3) and maternal grandmother (I.1). Each line corresponds to an individual cloned DNA fragment and each circle represents a CpG dinucleotide. Methylated CpGs are indicated by filled circles and unmethylated CpGs by open circles. Parental alleles were distinguished by the rs179436 nucleotide polymorphism for the 2,510,680-2,510,907 CpG island and the rs2074247 nucleotide polymorphism for the 2,511,982-2,512,194 CpG island. The 16 and 17 CpG islands are framed.

Figure 4: ICR1 deletions in BWS patients with ICR1 gain of methylation

(**A**) Graphical overview of log R ratio results focused at ICR1 obtained from the SNP array in BWS cases H50P and H63P; location of deletions identified by log R ratio values are underlined with a black arrow. (**B**) Pedigree of the familial H63P BWS case and segregation. Subjects identified in grey developed Wilms tumors. (**C**) Agarose gel of PCR amplifications (position 1,976,966 to 1,981,302 bp) showing maternally-inherited deletions in H50P and H63P families. (**D**) Genomic real-time PCR quantification assay at two loci within the ICR1 domain confirmed the deletions in patients H50P and H63P. (**E**) Position of the breakpoints of H63P's deletion (at 1,978,248 -1,978,293 bp and 1,980,488-1,980,533 bp) have been identified after sequencing both alleles and are highlighted on the chromatograms. The deletion removes three CTCF binding sites (2, 3 and 4). (**F**) Localization of ICR1 deletions identified in this study and deletions previously described [15-17].

Figure 5: Runs of homozygosity identified in control subjects and patients. Vertical lines represent length of homozygous regions. The black, light blue, dark blue and red colors represent control subjects, BWS patients with ICR1 gain of methylation, BWS patients with ICR2 loss of methylation and SRS patients with a loss of methylation, respectively. The A light grey box underlines the region encompassing the paternally-imprinted *ASCL2* gene. The B dark grey box underlines the region encompassing the *C11ORF21* and *TSPAN32* genes.

Supplementary figure 1: Schematic diagram of the 11p15 region with a summary of the duplications identified in the cohort and duplications previously described [12, 33, 34, 38].

Table 1: Clinical and molecular features of patients with Beckwith-Wiedemann syndrome

	BWS with ICR2 loss of methylation	BWS with ICR1 gain of methylation
n	78	35
sex F/M	36/42	17/18
gestational age[a], weeks mean ± SD; (range)	36.2 ± 3.2 (27-41)	36.7 ± 3.1 (30-40)
ART, n	9	1
monozygotic twins	7	0
fetal cases	6	3
familial cases	1	4[c]
phenotype		
macrosomia at birth[b], n (%)	31/65 (48%)	24/35 (69%)
birth weight (SDS)	1.7 ± 1.6	2.8 ± 1.9
macroglossia, n (%)	75/77 (97.5%)	31/33 (94%)
abdominal wall defect, n (%)	54/77 (70%)	20/32 (62%)
diastasis recti, n (%)	4	12
umbilical hernia, n (%)	21	7
exomphalos, n (%)	29	1
organomegaly, n (%)	33/69 (48%)	24/32 (75%)
body asymmetry, n (%)	20/71 (28%)	12/33 (36%)
hypoglycaemia, n (%)	26/63 (41%)	9/30 (30%)
ear abnormalities, n (%)	54/74 (73%)	9/30 (30%)
tumour, n (%)	0/71 (0%)	8/32 (25%)[d]
others		
ICR1 MI, mean ± (SD) (N=53.9 ± 2%)	52.8 ± 4.1	76 ± 10.3
ICR2 MI, mean ± (SD) (N=51.6 ± 2.5%)	8.5 ± 7.7	47.9 ± 3.8
parental DNA, n(%)	62/78 (79.5%)	18/35 (51%)
Both parents	57	14
One parent	5	4

a: gestational age is in weeks of amenorrhea
b: twins not included
c: 4 subjects from 2 families (two siblings in one family and a son and his mother in the other family)
d: all tumors were Wilms tumors
ART: assisted reproductive technology; MI: methylation index

Table 2: Clinical and molecular features of patients with Silver-Russell syndrome

	SRS with ICR1 loss of methylation
n	72
sex F/M	25/47
gestational age[a], weeks	38.2 ± 2
ART, n	6
monozygotic twins	3
phenotype	
IUGR, n (%)	66/68 (97%)
birth weight (SDS)[b]	-3.1 ± 0.7
post-natal growth retardation, n (%)	61/64 (95%)
relative macrocephaly at birth, n (%)	59/62 (95%)
facial dysmorphy, n (%)	49/57 (86%)
body asymmetry, n (%)	51/68 (75%)
feeding difficulties, n (%)	47/63 (75%)
severe, n	16
moderate, n	31
BMI (SDS)	-2.2 ± 1.1
BMI ≤ -2 SDS	40/59 (69%)
developmental delay, n (%)	9/57 (16%)
clinodactyly, n (%)	51/61 (84%)
others	
ICR1 MI, mean ± (SD) (N=53.9 ± 2%)	23 ± 8.3
ICR2 MI, mean ± (SD) (N=51.6 ± 2.5%)	47.6 ± 4.1
parental DNA, n(%)	30 (39%)
both parents	22
one parent	8

a: gestational age is in weeks of amenorrhea
b: twins not included
ART: assisted reproductive technology; IUGR: intrauterine growth retardation; MI: methylation index

Table 3: Copy number variations detected in SRS and BWS patients with cnvPartition v2.4.4 and QuantiSNP v2.3 softwares

patients	patients' group	CNV type	origin	parental chromosome	size kb	markers n	detection cnvPartition/ confidence score	detection QuantiSNP / Log Bayes Factor	qPCR validation
H4P	BWS ICR1	duplication	NA*	/	22	15	yes/45.74	no	no
H47P	BWS ICR1	duplication	*de novo*	paternal	400**	526	yes/1900.99	yes/30.33	yes
L65P	BWS ICR2	duplication	inherited	maternal	50	78	yes/232.11	yes/63.94	yes
L263P	BWS ICR2	deletion	*de novo*	maternal	4.4	3	yes/73.93	no	no
S63P	SRS ICR1	deletion	*de novo*	paternal	4	3	yes/230.73	no	no
S72P	SRS ICR1	duplication	inherited	maternal	80**	89	yes/398.29	yes/44.24	yes

* NA: parental DNA not available

** These CNVs include the most telomeric probe of the OPA.

BWS ICR1: BWS patients with ICR1 gain of methylation. BWS ICR2: BWS patients with ICR2 loss of methylation. SRS ICR1: SRS patients with ICR1 loss of methylation.

Table 4: Characterization of ICR1 deletions in BWS patients with ICR1 gain of methylation

	familial history	size (bp)	breakpoints	fused repeats	deleted CTCF binding sites
H32P	no	1834	1978828-1978846/1980662-1980680	B6/B3	2, 3
H50P	no	1834	1978576-1978605 /1980411-1980431	B6/B3	3, 4
H63P	yes	2240	1978248 -1978293/1980488-1980533	B6/B2	2, 3, 4

* Genomic positions were assigned according to the data provided by the UCSC genome browser (hg18, NCBI 36)

Supplementary table 1: Additional primers used in this study

Name	Localization hg18 (bp)	Sequence forward	Sequence reverse	Use
hg18_chr11_499934/500052	499934-500052	GAAGTATTCCCACCCCCAGT	CAGATCTGTGTGGAGCAGGA	CNV validation H47P, qPCR
hg18_chr11_1000151/1000289	1000151-1000289	TCCCAGCTGTTCCTCTCTGT	TGCAGCACTAACCACACACA	CNV validation H47P, qPCR
hg18_chr11_1499784/1499923	1499784-1499923	TCTAAGGCTTGGGGTTTTCC	ACAGCTCGTCCCGTAGAAGA	CNV validation H47P and S72P, qPCR
hg18_chr11_1960213/1960314	1960213-1960314	GAGGCAAGATTTGGAAACGA	CTGGGCAGGAGACTCTGATT	CNV validation H47P and S72P, qPCR
hg18_chr11_1977096/1977030	1977096-1977030	ACGTGGAGAGGTGAATTTGC	TCCTGCTCCAGGCATTGT	CNV validation H47P and S72P, qPCR
hg18_chr11_2123897/2124137	2123897-2124137	AAACCCACATTCCACAGAGG	TCTGAGGACCCTTGGAGAAA	CNV validation H47P, qPCR
hg18_chr11_2370152/2370254	2370152-2370254	GGCAGAAGCAGAGGTCACA	ACACCATGCAGGTCAGACAC	CNV validation H47P, qPCR
hg18_chr11_2375108/2375201	2375108-2375201	CCTTCATGCACCTGTCCTTT	GCATGCCTGATGTTCCTTCT	CNV validation H47P, qPCR
hg18_chr11__2155877/2156345	2155877-2156345	AGGGAAGGGGATCCAGTG	CAGACACAGACCAGCGAAAA	CNV validation H47P, Parental origin
hg18_chr11_2371018/2371497	2371018-2371497	CTGCTGAGGGATAGGGGAGT	AGTGGCATCAGAAGGCACAG	CNV validation H47P, Parental origin
hg18_chr11_2191887/2192349	2191887-2192349	GTTCCTCCTGCCTCCCTAAC	AGAGCGGGGAAGAAACAGAT	CNV validation H47P, Parental origin
hg18_chr11_2035226/2035462	2035226-2035462	CCTCGATAGCCATTTTGCAT	GCATGGCAAAAGGAGAAAAG	CNV validation S72P, qPCR
hg18_chr11_2107371/2107558	2107371-2107558	GCTTCTGGGTCCTGGTGAC	CTCGAAGCGTTTTGGATCTC	CNV validation S72P, qPCR
hg18_chr11_1980297/1980616	1980297-1980616	AGGTGTTTTAGTTTTTTGGATGATA	CCATAAATATTCTATCCCTCACTA	CNV validation S72P, Bisulfite treatment
hg18_chr11_2486398/2486518	2486398-2486518	AGGACCCAGACTCCCAGAC	AGGTGGTCACTGCCATCTTC	CNV validation L65P, qPCR
hg18_chr11_2540424/2540567	2540424-2540567	CTGTGTCCACCCCTCTTCAG	ACTTAGGCCTGGGGACCTT	CNV validation L65P, qPCR
hg18_chr11_2526198/2526347	2526198-2526347	TCGGTCAGGTTAGTTGCTGT	CCCCCAGAGCTTAGGACACT	CNV validation L65P, qPCR
hg18_chr11_2472491/2472581	2472491-2472581	GAAGCCCACTTGATCACCAT	GAGCACCGATGCAAAAATCT	CNV validation L65P, qPCR
hg18_chr11_2676672/2677949	2676672-2677949	TGGGACCCCAACTACTCAGA	AGGACACGGCACATCACTTT	CNV validation L65P, sequencing
hg18_chr11_2677793/2679793	2677793-2679793	ACCGTTCTGCCTGGAGACTG	GCCACCCTCAACTCAACATT	CNV validation L65P, sequencing
hg18_chr11_2510633/2510968	2510633-2510968	GGTTTTTGATTTTAGTAGAGGGAGG	AAACAAAAACTCCCTAAAAACACAT	CNV validation L65P, Bisulfite treatment
hg18_chr11_2511951/2512483	2511951-2512483	AGTGAGATTTTGTAGGGAGTTTTTG	AACCCACAAAAAAACACAACTCT	CNV validation L65P, Bisulfite treatment
hg18_chr11_2674923/2675237	2674923-2675237	GGAGTAGGCCAAGGATGTCA	GAGTTTTCCAGAGGCAGCAC	deletion ICR2 L65P, qPCR
hg18_chr11_2649043/2649262	2649043-2649262	GACCTCAAAATCCGATGTCC	GGTTGCTCTTCTGCCTGCTA	deletion ICR2 L65P, qPCR
hg18_chr11_1978454/1978696	1978454-1978696	ATGTGGCTCCCATGAATGTC	GGCTCTTGCATAGCACATGA	deletions ICR1 H50P and H63P, qPCR
hg18_chr11_1979289/ 1979612	1979289-1979612	CTGATTCCAGCAGCACAGAG	TCAGTGCAGGTTTGAGATGC	deletions ICR1 H50P and H63P, qPCR
hg18_chr5_134898593/134898695	134898593-134898695	GCTCTCTGACCCCAGTAGCC	TGTGTGGAGCAAGTCTTTGG	housekeeping gene, qPCR

Supplementary table 2: Runs of homozygosity detected in control subjects and patients

Sample id.	Start Position (bp)	End Position (bp)	Length (bp)	Probes (n)	Score Max. Log BF
Control samples					
CS_107	2264880	2381611	116732	210	37.1696
CS_154	2155554	2261555	106002	195	32.2554
CS_187	2559602	2690701	131100	195	34.3885
CS_189	2283188	2381611	98424	168	30.3942
CS_19	2128498	2346891	218394	408	101.166
CS_205	2128498	2261555	133058	257	45.1774
CS_245	2159621	2261078	101458	185	35.3047
CS_254	2155554	2262744	107191	199	33.8643
CS_300	2155554	2347625	192072	349	62.0078
CS_300	2780921	2869522	88602	176	42.9269
CS_315	2233543	2381611	148069	278	37.1292
CS_365	2233543	2529468	295926	507	62.7432
CS_370	2707910	2816117	108208	207	38.2093
CS_375	2264880	2381611	116732	210	40.529
CS_415	2412354	2537338	124985	188	37.1774
CS_7	2156905	2267446	110542	205	30.2087
CS_D	2165989	2381611	215623	394	59.2346
ICR1 GOM BWS					
AA30P	2283727	2479634	195908	302	32.303
H12P	2286571	2381611	95041	158	30.3052
H20P	2285283	2381284	96002	161	34.5552
H23P	2283727	2425532	141806	239	33.3802
H29P	2176538	2387096	210559	381	72.3474
H2P	2151386	2261555	110170	203	42.128
H2P	2291307	2387096	95790	159	39.9038
H43P	1970084	2177516	207433	358	78.7391
H43P	2273296	2389540	116245	209	49.8905
H43P	2409470	2597296	187827	290	61.554
H44P	2156905	2381611	224707	407	90.1299
H54P	2181257	2267728	86472	156	40.1736
H55P	2206725	2381611	174887	312	43.1212
H61P	2283727	2385251	101525	172	31.1806
H61P	2644661	2782775	138115	264	53.5701
H69P	2511521	2708236	196716	304	40.6492
H6P	2047032	2381611	334580	592	152.827
H70P	2505433	2690701	185269	289	39.761
H8P	2144814	2261555	116742	217	49.5353
ICR2 LOM BWS					
41P	2138346	2381611	243266	449	91.8929
41P	2423780	2597296	173517	269	31.3046
L101P	2156905	2381611	224707	406	88.2207
L110P	2073262	2261555	188294	344	78.5962
L113P	2191119	2387441	196323	342	71.585
L116P	2206725	2381284	174560	312	45.4417
L119P	2497741	2720353	222613	354	65.004
L134P	2582824	2751568	168745	270	34.6159
L138P	2716781	2869522	152742	295	52.1911
L151P	2173007	2262744	89738	167	31.3149
L164P	2165989	2381284	215296	393	75.3495
L167P	2399757	2584063	184307	290	54.5854
L170P	2150393	2272679	122287	226	50.2314
L173P	2285283	2388145	102863	175	35.2167
L177P	2283188	2387096	103909	179	35.2186
L177P	2559602	2720353	160752	248	40.4669
L186P	2185285	2387096	201812	363	60.9426

L190P	2264880	2387096	122217	221	44.6633
L196P	2264880	2387096	122217	221	45.4819
L1P	2156905	2347625	190721	346	47.3695
L203P	2264880	2388145	123266	223	41.479
L20P	2283188	2387096	103909	179	33.5019
L214P	2250529	2529468	278940	472	101.227
L246P	2283727	2381611	97885	166	30.5518
L262P	2270670	2381611	110942	200	35.9644
L278P	2250529	2381611	131083	244	49.4586
L39P	2126011	2261555	135545	266	38.9765
L39P	2393143	2505833	112691	169	33.0644
L42P	2168253	2381611	213359	390	72.101
L49P	2176538	2267728	91191	168	30.8099
L4P	2000375	2191705	191331	332	44.9354
L4P	2233543	2381611	148069	278	36.2062
L4P	2652083	2764038	111956	206	39.2673
L58P	2176538	2288613	112076	220	46.4965
L95P	2039703	2262744	223042	386	111.035
ICR1 LOM SRS					
S103P	2049559	2192166	142608	263	63.3619
S41P	2060139	2177516	117378	217	55.3193
S29P	2104733	2192830	88098	203	32.0159
S5P	2130774	2261555	130782	252	48.5926
S122P	2133080	2241585	108506	207	36.0915
S129P	2137348	2246000	108653	205	30.2934
S72P	2149268	2261555	112288	208	42.3326
S116P	2155554	2261555	106002	194	41.4788
S107P	2156905	2267446	110542	205	46.4942
S21P	2156905	2425532	268628	480	118.579
S75P	2156905	2261555	104651	192	45.9219
S121P	2159621	2262915	103295	192	44.5157
S115P	2165989	2292816	126828	250	65.862
S104P	2191119	2387096	195978	341	74.2499
S120P	2191119	2308917	117799	218	50.8112
S123P	2233543	2385251	151709	284	68.3263
S38P	2233543	2440576	207034	372	67.4105
S95P	2233543	2387096	153554	289	49.5405
S41P	2242435	2445918	203484	358	79.6654
S18P	2253669	2381284	127616	234	42.2847
S127P	2264880	2405095	140216	253	52.8612
S84P	2264880	2425532	160653	281	68.3503
S32P	2270670	2426669	156000	276	36.1267
S20P	2276509	2385251	108743	194	32.2157
S88P	2281815	2385251	103437	178	31.6654
S117P	2283727	2384402	100676	171	38.3117
S60P	2283727	2387096	103370	176	38.4677
S20P	2409470	2594837	185368	286	33.6277
S120P	2423780	2543930	120151	187	39.6514

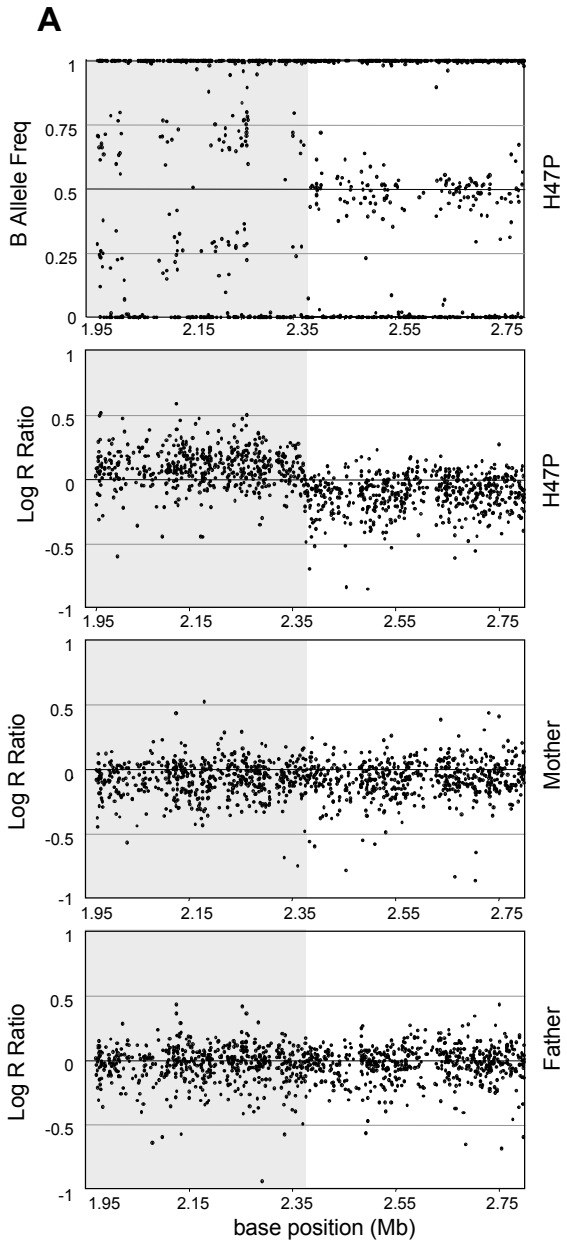
A
B Allele Freq
Log R Ratio
H47P
Mother
Father
base position (Mb)

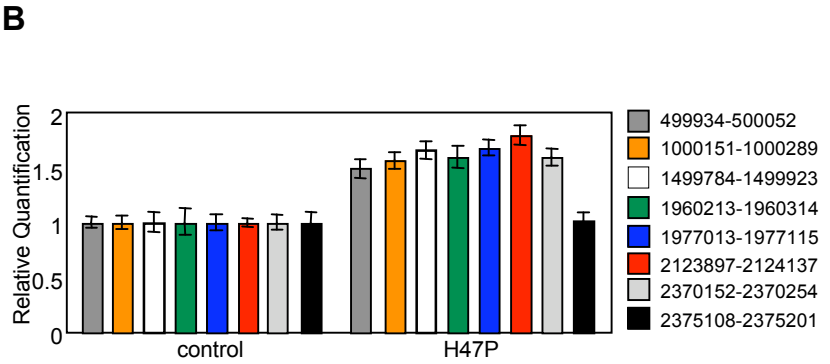
B
Relative Quantification
control
H47P
499934-500052
1000151-1000289
1499784-1499923
1960213-1960314
1977013-1977115
2123897-2124137
2370152-2370254
2375108-2375201

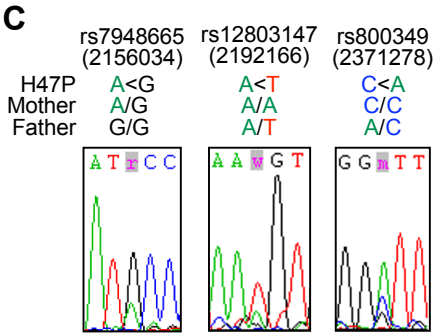
C
rs7948665 (2156034)
rs12803147 (2192166)
rs800349 (2371278)
H47P A<G A<T C<A
Mother A/G A/A C/C
Father G/G A/T A/C

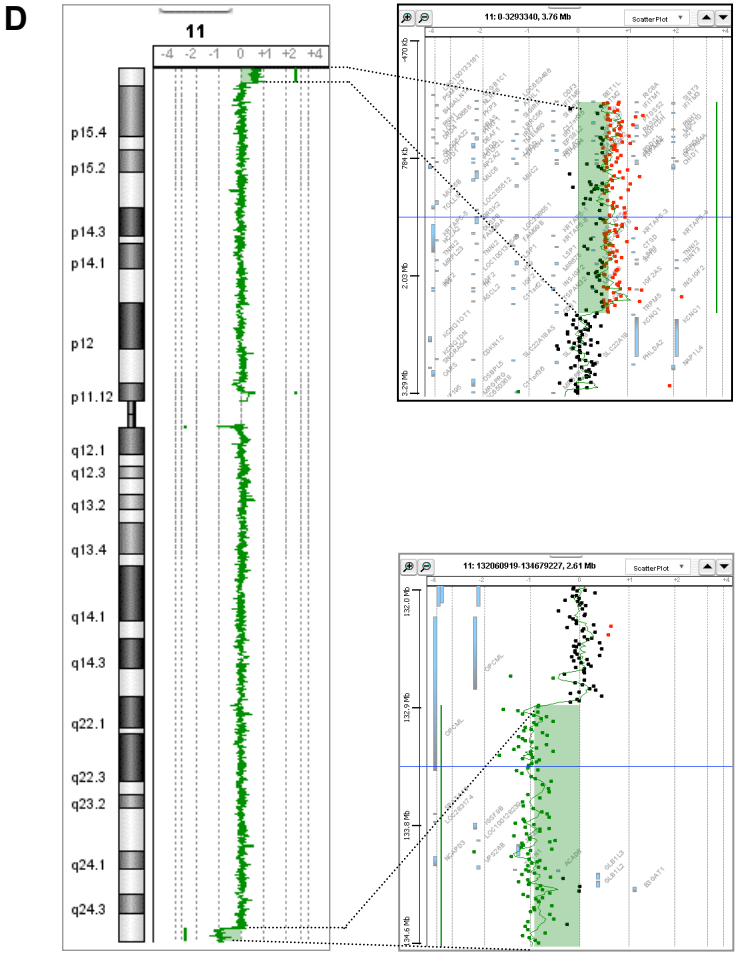
D
11

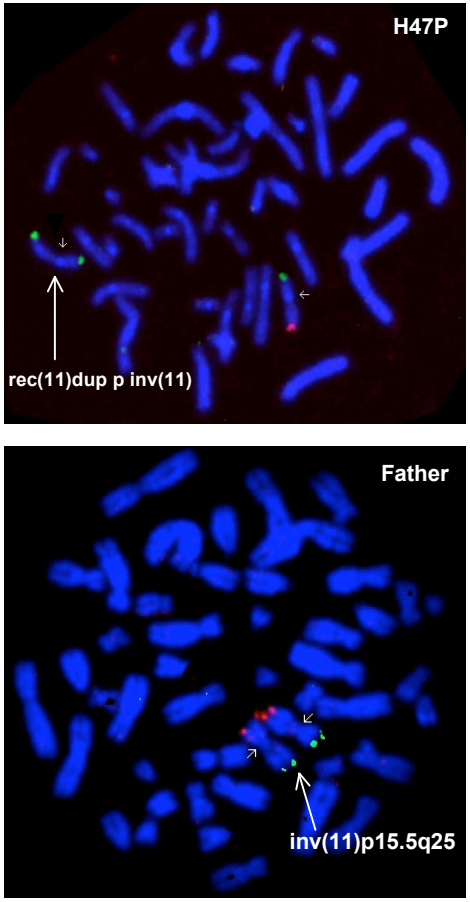
E
H47P
rec(11)dup p inv(11)
Father
inv(11)p15.5q25

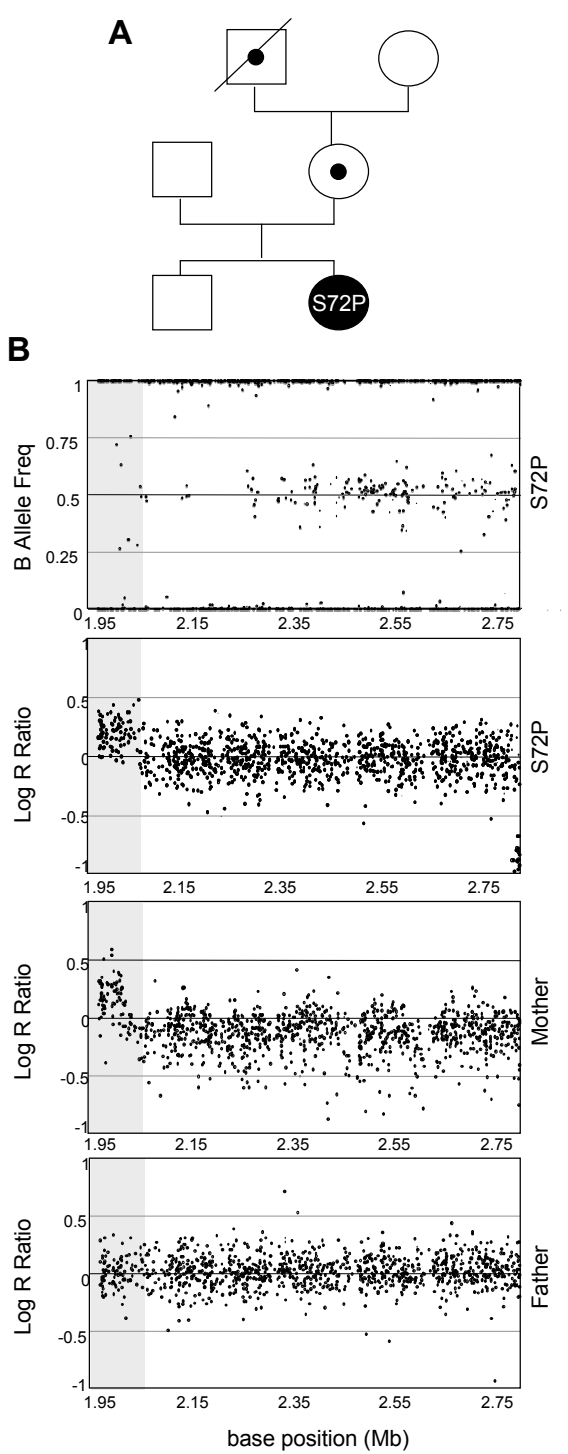
A
S72P
B
B Allele Freq
Log R Ratio
Log R Ratio
Log R Ratio
S72P
S72P
Mother
Father
1.95
2.15
2.35
2.55
2.75
base position (Mb)

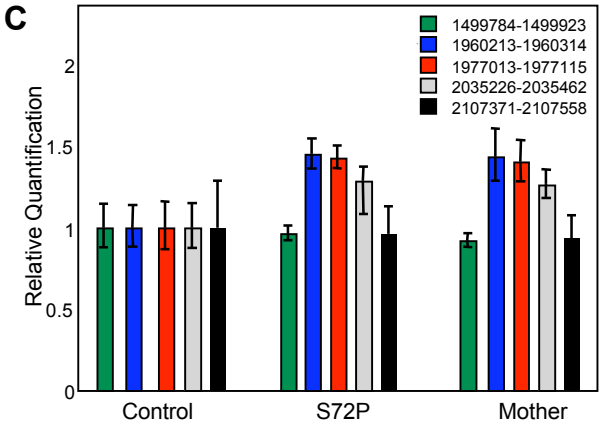
C
1499784-1499923
1960213-1960314
1977013-1977115
2035226-2035462
2107371-2107558
Relative Quantification
Control
S72P
Mother

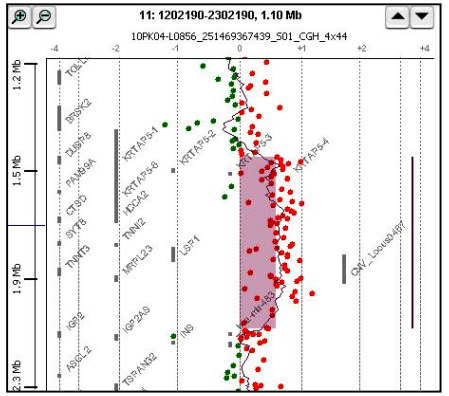
D
11: 1202190-2302190, 1.10 Mb
10PK04-L0856_251469367439_S01_CGH_4x44

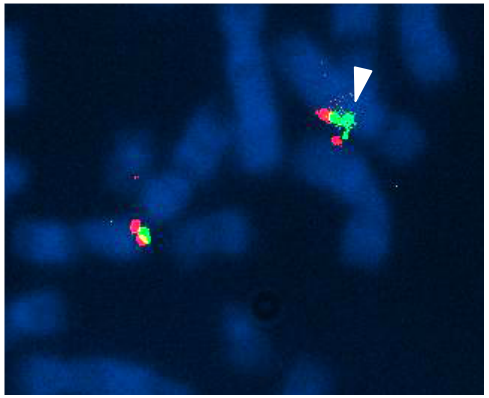
E

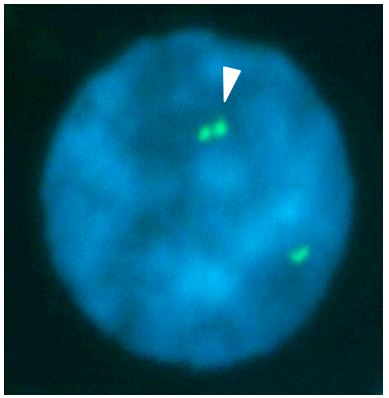
F

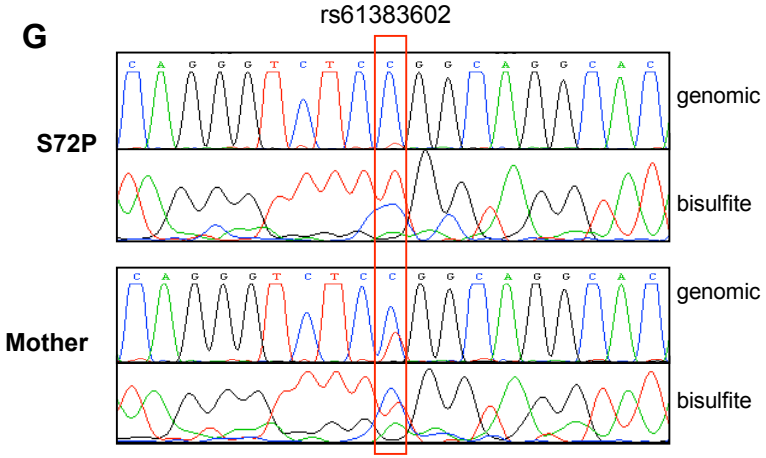
G
rs61383602
S72P
genomic
bisulfite
Mother
genomic
bisulfite

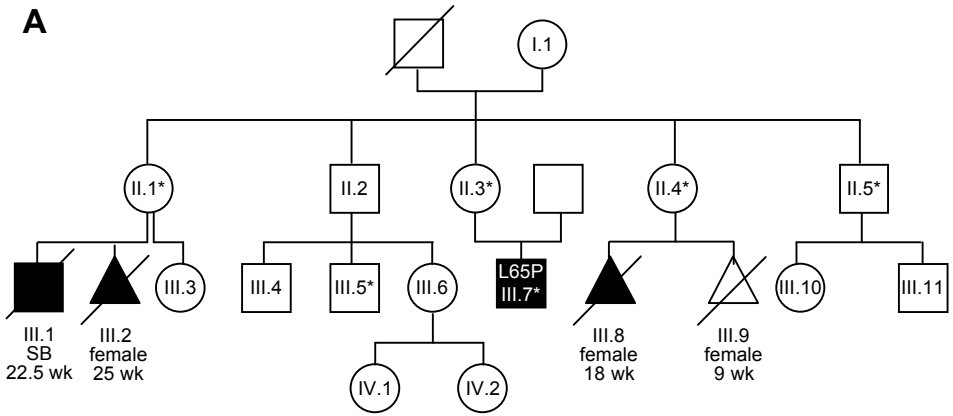
A
I.1
II.1*
II.2
II.3*
II.4*
II.5*
III.1
SB
22.5 wk
III.2
female
25 wk
III.3
III.4
III.5*
III.6
L65P
III.7*
III.8
female
18 wk
III.9
female
9 wk
III.10
III.11
IV.1
IV.2

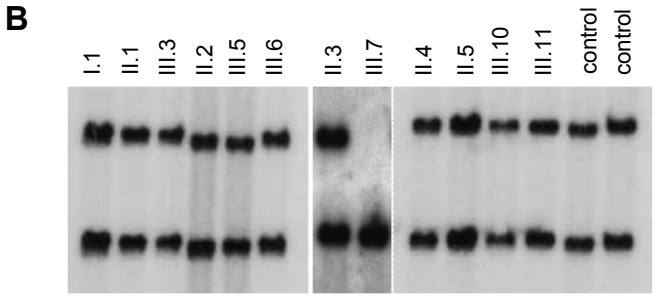
B
I.1
II.1
III.3
II.2
III.5
III.6
II.3
III.7
II.4
II.5
III.10
III.11
control
control

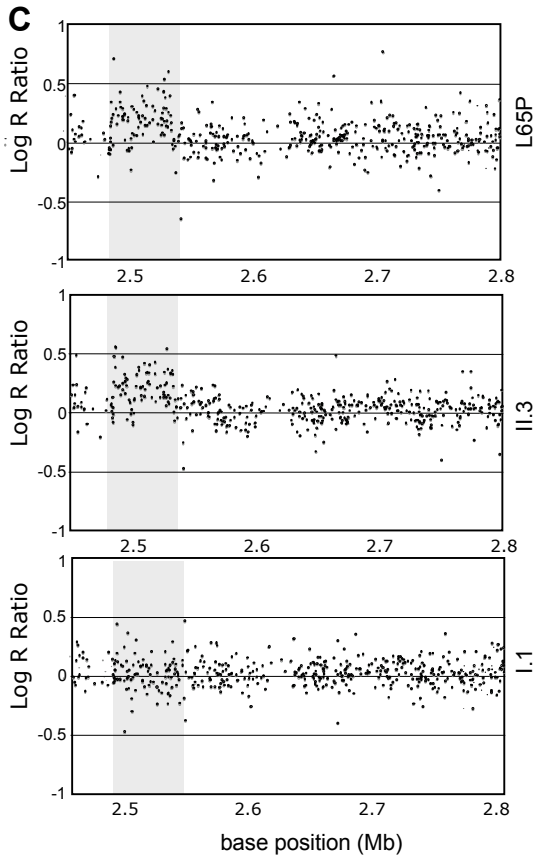
C
Log R Ratio
L65P
II.3
I.1
base position (Mb)

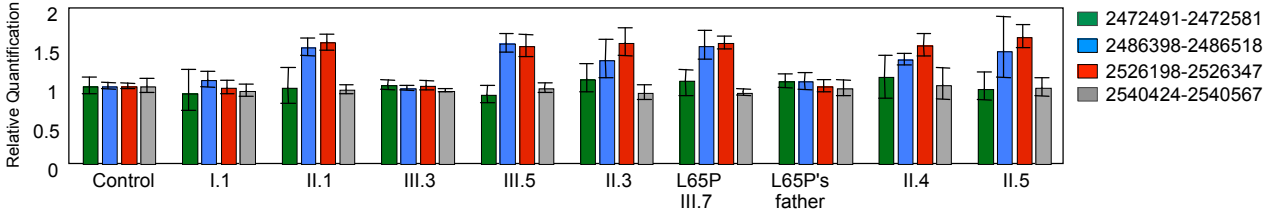
D
Relative Quantification
Control
I.1
II.1
III.3
III.5
II.3
L65P
III.7
L65P's
father
II.4
II.5
2472491-2472581
2486398-2486518
2526198-2526347
2540424-2540567

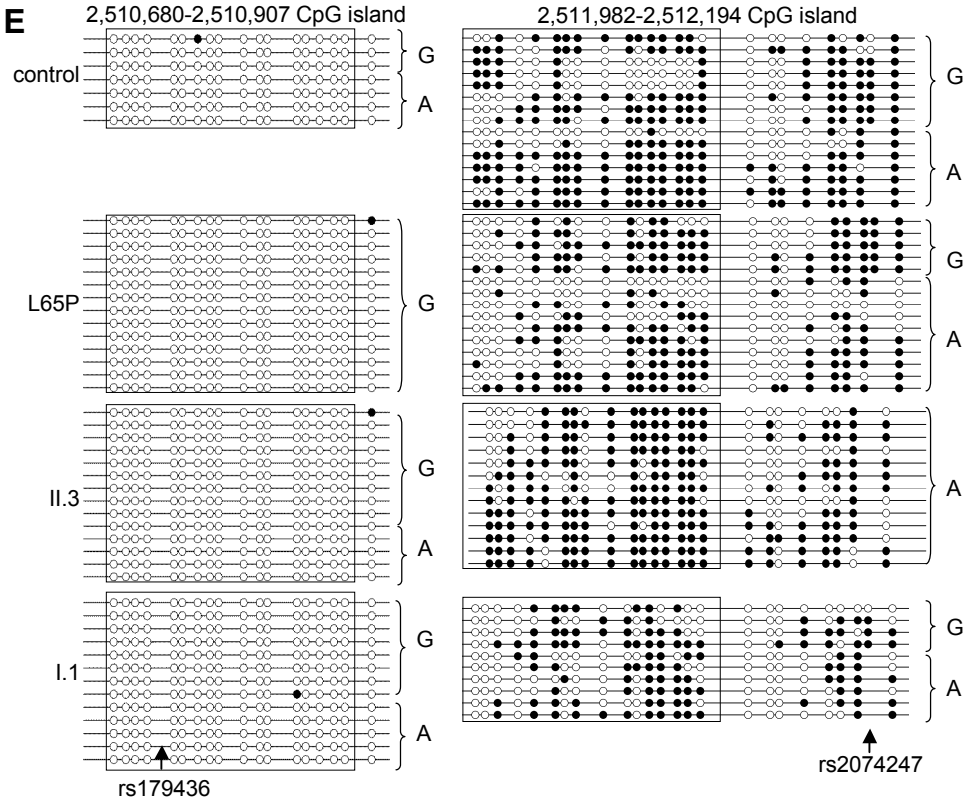
E
2,510,680-2,510,907 CpG island
2,511,982-2,512,194 CpG island
control
L65P
II.3
I.1
G
A
rs179436
rs2074247

Fig 3

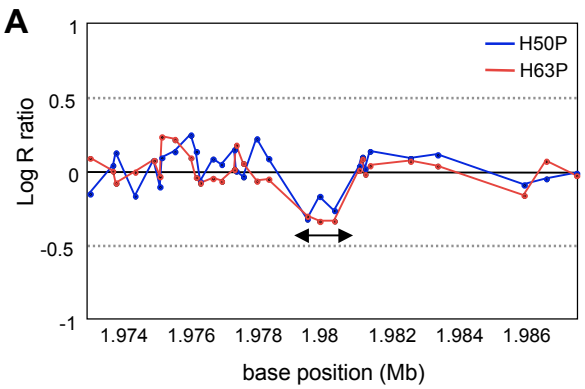
A
H50P
H63P
Log R ratio
1
0.5
0
-0.5
-1
1.974
1.976
1.978
1.98
1.982
1.984
1.986
base position (Mb)

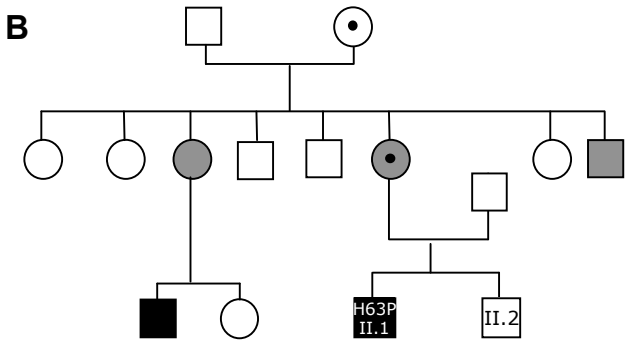
B
H63P
II.1
II.2

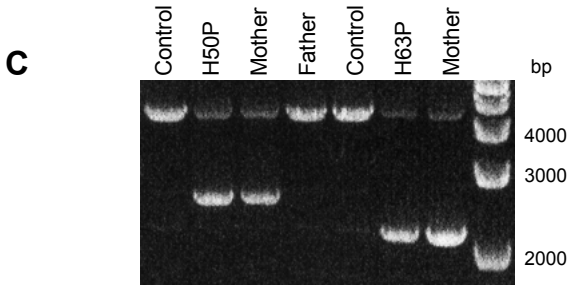
C
Control
H50P
Mother
Father
Control
H63P
Mother
bp
4000
3000
2000

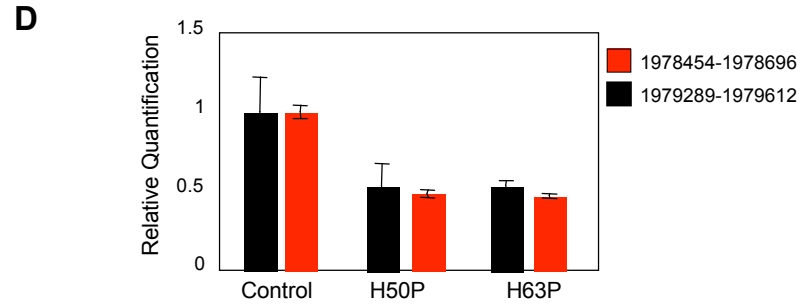
D
Relative Quantification
1.5
1
0.5
0
1978454-1978696
1979289-1979612
Control
H50P
H63P

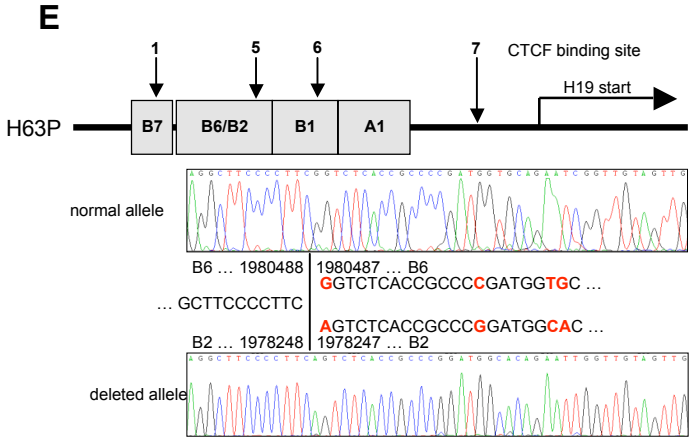
E
1
5
6
7
CTCF binding site
H19 start
H63P
B7
B6/B2
B1
A1
normal allele
B6 … 1980488
1980487 … B6
GGTCTCACCGCCCCGATGGTGC …
… GCTTCCCCTTC
AGTCTCACCGCCCGGATGGCAC …
B2 … 1978248
1978247 … B2
deleted allele

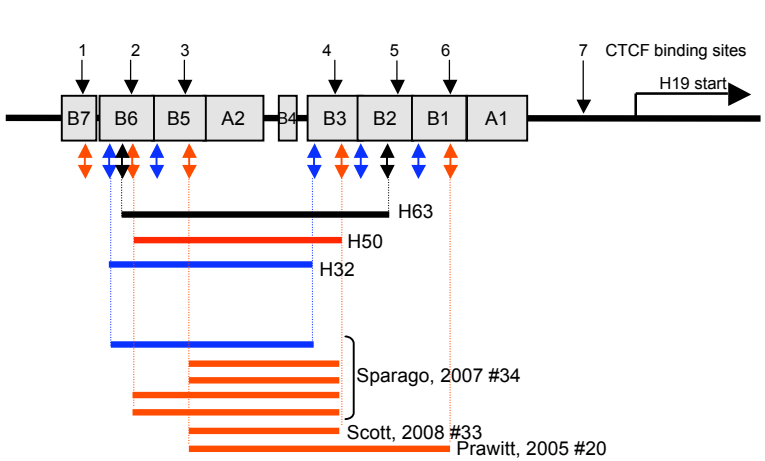
F
1
2
3
4
5
6
7
CTCF binding sites
H19 start
B7
B6
B5
A2
B4
B3
B2
B1
A1
H63
H50
H32
Sparago, 2007 #34
Scott, 2008 #33
Prawitt, 2005 #20

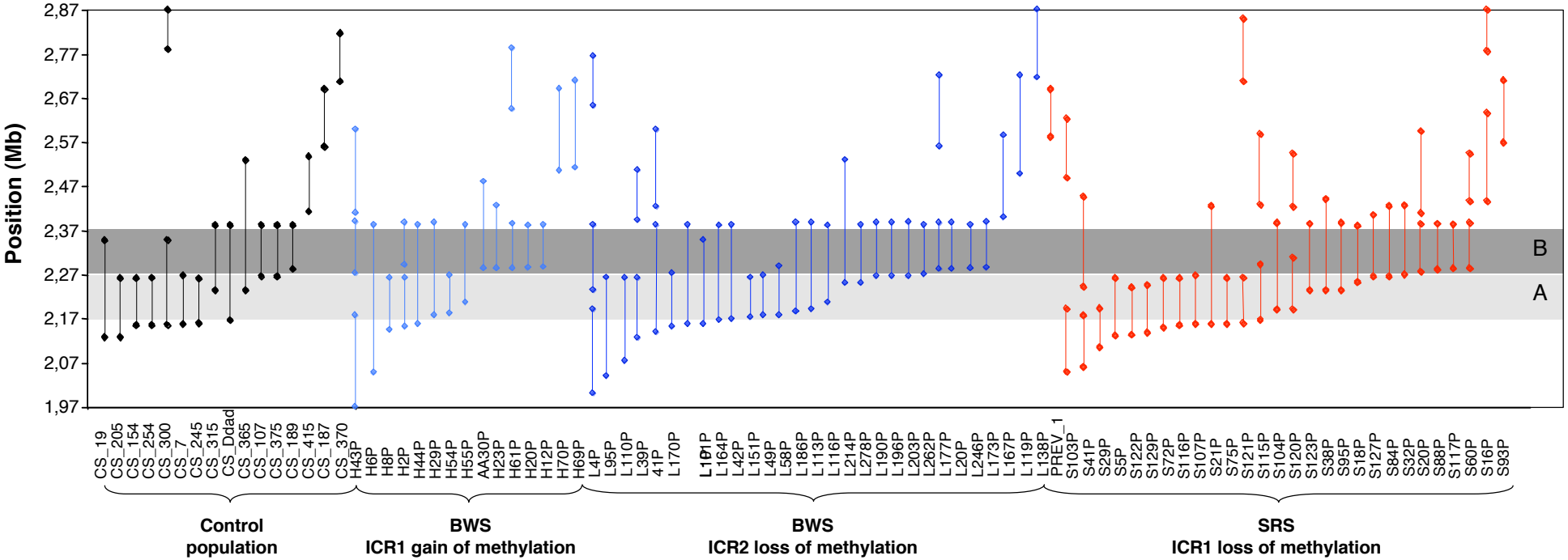
Position (Mb)
2,87
2,77
2,67
2,57
2,47
2,37
2,27
2,17
2,07
1,97
B
A
CS_19
CS_205
CS_154
CS_254
CS_300
CS_7
CS_245
CS_315
CS_Ddad
CS_365
CS_107
CS_375
CS_189
CS_415
CS_187
CS_370
H43P
H6P
H8P
H2P
H44P
H29P
H54P
H55P
AA30P
H23P
H61P
H20P
H12P
H70P
H69P
L4P
L95P
L110P
L39P
41P
L170P
L164P
L42P
L151P
L49P
L58P
L186P
L113P
L116P
L214P
L278P
L190P
L196P
L203P
L262P
L177P
L20P
L246P
L173P
L167P
L119P
L138P
PREV_1
S103P
S41P
S29P
S5P
S122P
S129P
S72P
S116P
S107P
S21P
S75P
S121P
S115P
S104P
S120P
S123P
S38P
S95P
S18P
S127P
S84P
S32P
S20P
S88P
S117P
S60P
S16P
S93P
Control population
BWS ICR1 gain of methylation
BWS ICR2 loss of methylation
SRS ICR1 loss of methylation

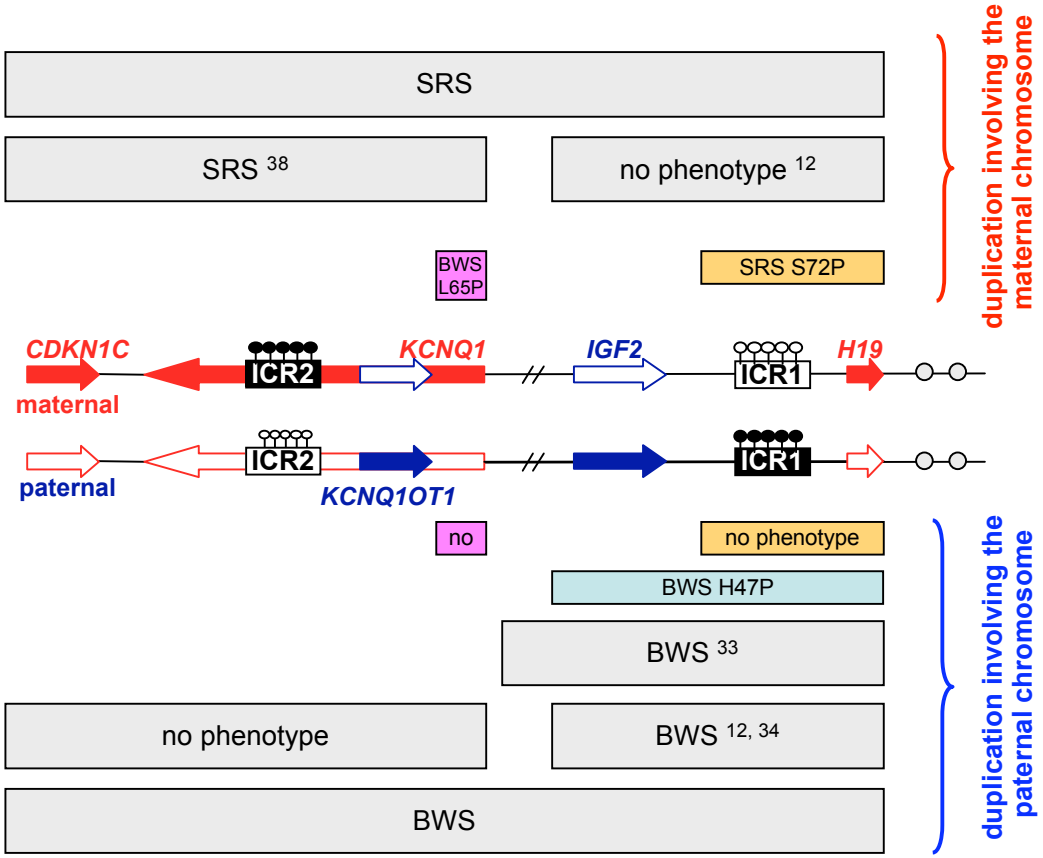
SRS
SRS 38
no phenotype 12
BWS L65P
SRS S72P
duplication involving the maternal chromosome
CDKN1C
ICR2
KCNQ1
IGF2
ICR1
H19
maternal
ICR2
ICR1
paternal
KCNQ1OT1
no
no phenotype
BWS H47P
BWS 33
no phenotype
BWS 12, 34
BWS
duplication involving the paternal chromosome

Suppl fig 1